

Fault Detection in Multimode Processes Through Improved Nonlinear External Analysis Regression

RONGRONG SUN 

College of Information Science and Engineering, Northeastern University, Liaoning 110819, China

e-mail: neuronrong@hotmail.com

This work was supported by the National Natural Science Foundation of China under Grant 61733003.


ABSTRACT External analysis serve as a cogent approach for multimode process detection in recent years. However, external analysis approach may not detect faults well because of the imprecise extraction of relations between variables. This paper proposes a fault detection approach for multimode processes, called improved nonlinear external analysis regression. External regression models between external variables and main/quality variables are established to remove mode-change-related information in the main/quality variables, ensuring that the following work is performed under a single mode. The remaining information in the main and quality variables is employed to develop an internal regression model for fault detection. Compared with existing approaches, the proposed approach has the following advantages: (1) In external regression models, applying kernel orthogonal projections to latent structures resulted in a relatively smaller number of loadings, reduced model complexity and, not least, efficient extraction of mode-change-related information in main and quality variables. (2) Internal regression model has the capacity to improve separation performance of output-related information and output-unrelated information. (3) Two comprehensive and perspicuous detection statistics are designed to accurately detect process faults. To experimentally verify the stability and superiority of the method, it is applied to a penicillin fermentation process for fault detection.

INDEX TERMS Fault detection, kernel orthogonal projections to latent structures, improved nonlinear external analysis regression, penicillin fermentation process, multimode processes.

I. INTRODUCTION

In recent years, to minimize cost and maximize profit, multimode production has become increasingly popular, while processes are getting more and more complex. Hence, process detection, which plays an important role in ensuring production safety, for multimode processes is particularly important. Multivariate statistical techniques [1]–[8], such as the principal component analysis (PCA) and partial least squares (PLS), have been integrated into multimode methods to extract statistical characteristics of different modes for effective process detection [9]–[12]. As a result, some effective approaches have been obtained, such as global models [13]–[15], mixture models [16]–[18], multiple models [19] and adaptive models [20], [21].

For a global model, the common subspace model is established to achieve multimode process detection, which has limitation in describing each operating mode due to inaccurate extraction of statistical characteristics. On the basis of which,

The associate editor coordinating the review of this manuscript and approving it for publication was Ali Salehzadeh-Yazdi .

multiple models and mixture models were adopted. Particularly, Zhao *et al.* [22], [23] proposed multiple PCA models and multiple PLS models based on similarities between any two models. A comprehensive subspace decomposition by between-mode relative analysis was developed to check the specific changes of variables from one mode to another [24]. Bayesian inference-based finite Gaussian mixture models were proposed to solve a multimodal distribution of multimode processes [25]. On the other hand, some adaptive multimode models such as mode clustering, unfolding, and piecewise linear model were developed to achieve the fault detection of dynamic or nonlinear multimode processes [26]–[28]. In addition, hidden Markov models have also been considered in recent years because of their strong theoretical and stochastic features [29], [30].

As a mode change is due to different operating conditions that are often determined by mode-change-related variables, it can be eliminated by removing the mode-change-related variables and their influence on the other variables. Hereby, an external analysis-based method [31] was proposed. Ge *et al.* [32] developed a nonlinear external analysis method

for online monitoring. However, the correlation between main and quality variables has not been considered. Then, an external analysis-based regression model [33] was constructed for robust soft sensing, in which principal component regression (PCR) [34], [35] and PLS were employed to construct the regression model. Remarkably, in reference [33], the corresponding nonlinear tools were introduced to resolve the nonlinear relationships although they were not described in detail. As a result, nonlinear external analysis regression (NEAR) model, such as kernel partial least square-based EAR (KPLS-EAR), could be established. However, for KPLS, there is some cross information between output-related and output-unrelated spaces, this reduces the accuracy of KPLS-EAR. Furthermore, although the shortcoming of KPLS can be resolved by some new nonlinear tools [36]–[41], due to different purposes of modeling, the characteristics of industrial data may not be accurately described if one existing nonlinear tool is utilized directly during all modeling phases.

Based on the above considerations, we propose a new multimode process detection approach by integrating kernel orthogonal projections to latent structures (KOPLS) and improved PLS (IPLS) [42] into external analysis, which we refer to as the improved NEAR (INEAR). A new external model–internal model–detection structure is designed to clearly show the model. The INEAR achieves the following objectives. First, two nonlinear external regression models based on KOPLS are established, with mode-change-related information in main and quality variables completely removed. Specifically, KOPLS is applied to analyze correlation between external variables and main variables, and then, the same is true for external variables and quality variables. Thus, the remaining information in the main and quality variables extracted by this method is more accurate than that extracted by KPLS-EAR. Second, one internal regression model based on IPLS is established, with output-related and output-unrelated information completely separated. The above external and internal analyses provide a simpler and more accurate model than the NEAR methods, especially KPLS-EAR. Finally, comprehensive and perspicuous detection statistics are designed to track process change, ensuring the accuracy of detection information. The proposed detection method is applied to a penicillin fermentation process (PFP), which has several operating modes, under varying initial conditions, set points, and/or pH, etc. The detection results show that the proposed method can improve the detection performance for PFP.

The rest of this paper is organized as follows. Section II briefly describes IPLS and KPLS-EAR. In Section III, details regarding INEAR are given. Section IV presents an online detection strategy. In Section V, the proposed method is applied to a PFP for model validation. Finally, the conclusions of this study are drawn in Section VI.

II. IPLS AND KPLS-EAR

In this section, IPLS is first described, following which the original NEAR (that is, KPLS-EAR) is given. IPLS is a

regression method that can accurately analyze the correlation between input and output. KPLS is integrated into external analysis to obtain the KPLS-EAR.

A. IPLS

For input matrix $\mathbf{X} \in \mathbf{R}^{n \times r}$ and output matrix $\mathbf{Y} \in \mathbf{R}^{n \times l}$, where n , r , and l represent the numbers of samples, process variables, and quality variables, respectively, IPLS [42] is given as follows:

Step 1: PLS is performed on \mathbf{X} and \mathbf{Y} to obtain the regression coefficient matrix \mathbf{V}

$$\mathbf{Y} = \mathbf{X}\mathbf{V} + \tilde{\mathbf{Y}} \quad (1)$$

Here, $\mathbf{X}\mathbf{V}$ and $\tilde{\mathbf{Y}}$ are the principal and residual information of \mathbf{Y} , respectively.

Step 2: Singular value decomposition (SVD) is performed on $\mathbf{V}\mathbf{V}^T$ as:

$$\mathbf{V}\mathbf{V}^T = [\mathbf{P}_1 \ \mathbf{P}_2] \begin{bmatrix} \Lambda & 0 \\ 0 & 0 \end{bmatrix} \begin{bmatrix} \mathbf{P}_1^T \\ \mathbf{P}_2^T \end{bmatrix} \quad (2)$$

Here, $\mathbf{P}_1 \in \mathbf{R}^{r \times q}$, $\mathbf{P}_2 \in \mathbf{R}^{r \times (r-q)}$, $\Lambda = \text{diag} \{ \lambda_1, \lambda_2, \dots, \lambda_q \}$, q is the number of nonzero singular values, and $\mathbf{P}_1\mathbf{P}_1^T$ and $\mathbf{P}_2\mathbf{P}_2^T$ are the projection matrices of \mathbf{X} .

Step 3: \mathbf{X} is projected onto the projection matrices:

$$\mathbf{X} = \hat{\mathbf{X}} + \tilde{\mathbf{X}} = \mathbf{X}\mathbf{P}_1\mathbf{P}_1^T + \mathbf{X}\mathbf{P}_2\mathbf{P}_2^T = \mathbf{T}_1\mathbf{P}_1^T + \mathbf{T}_2\mathbf{P}_2^T \quad (3)$$

Here, \mathbf{P}_1 and \mathbf{P}_2 are treated as the loading matrices of \mathbf{X} and $\tilde{\mathbf{X}}$, respectively; $\mathbf{T}_1 = \mathbf{X}\mathbf{P}_1$ and $\mathbf{T}_2 = \mathbf{X}\mathbf{P}_2$ are the score matrices of \mathbf{X} and $\tilde{\mathbf{X}}$, respectively; and $\hat{\mathbf{X}} = \mathbf{T}_1\mathbf{P}_1^T$ and $\tilde{\mathbf{X}} = \mathbf{T}_2\mathbf{P}_2^T$ are the output-related information and output-unrelated information, respectively.

Thus, orthogonal decompositions on \mathbf{X} and \mathbf{Y} are completed, and the IPLS model can be given as:

$$\begin{cases} \mathbf{X} = \mathbf{T}_1\mathbf{P}_1^T + \mathbf{T}_2\mathbf{P}_2^T \\ \mathbf{Y} = \mathbf{X}\mathbf{V} + \tilde{\mathbf{Y}} \end{cases} \quad (4)$$

To realize online detection, the corresponding detection statistics are established. For online data $\mathbf{x}_{new} \in \mathbf{R}^r$, the detection statistics are computed as:

$$\begin{cases} T_{\hat{\mathbf{x}}}^2 = \mathbf{t}_{\hat{\mathbf{x}}}^T \left[\mathbf{T}_1^T \mathbf{T}_1 / (n-1) \right]^{-1} \mathbf{t}_{\hat{\mathbf{x}}} \\ T_{\tilde{\mathbf{x}}}^2 = \mathbf{t}_{\tilde{\mathbf{x}}}^T \left[\mathbf{T}_2^T \mathbf{T}_2 / (n-1) \right]^{-1} \mathbf{t}_{\tilde{\mathbf{x}}} \end{cases} \quad (5)$$

Here, $\mathbf{t}_{\hat{\mathbf{x}}} = \mathbf{P}_1^T \mathbf{x}_{new}$ and $\mathbf{t}_{\tilde{\mathbf{x}}} = \mathbf{P}_2^T \mathbf{x}_{new}$ are new score vectors of the output-related subspace and output-unrelated subspace, respectively.

B. KPLS-EAR

Generally, a mode change is due to different operating conditions that are assumed to be related to outside of process. Variables that directly impact operating conditions are defined as external variables \mathbf{E} . Other variables are referred to as main variables \mathbf{X} and quality variables \mathbf{Y} [33]. Although the main and quality variables are not directly related to the

operating conditions, they may be influenced by external variables. Therefore, the external variables and the information in the main/quality variables influenced by external variables, should be eliminated as normal changes in the external variables are not considered as process faults. For the situation where nonlinear relations between variables exist in multimode processes, KPLS [43] is utilized to establish the KPLS-EAR model and detection scheme.

Modeling:

1) The regression model between \mathbf{E} and \mathbf{X} is employed using KPLS to obtain mode-change-unrelated information \mathbf{F}_x :

$$\mathbf{X} = \mathbf{TQ}^T + \mathbf{F}_x \quad (6)$$

Here, \mathbf{T} is the score matrix of $\Phi(\mathbf{E})$, \mathbf{Q} is the loading matrix of \mathbf{X} . \mathbf{F}_x is robust to mode change, that is, it is only sensitive to process faults. Thereby, it is appropriate to be analyzed to achieve effective detection information.

2) The same model between external variables and quality variables is employed to obtain mode-change-unrelated information \mathbf{F}_y .

3) KPLS is utilized to \mathbf{F}_x and \mathbf{F}_y to obtain the correlation between them.

Detection:

1) For the online data \mathbf{e}_{new} and \mathbf{x}_{new} , the mode-change-unrelated information in \mathbf{x}_{new} is computed as:

$$\tilde{\mathbf{x}}_{new} = \mathbf{x}_{new} - \hat{\mathbf{x}}_{new} = \mathbf{x}_{new} - \mathbf{QU}^T \mathbf{k}_{new} \quad (7)$$

Here, $\hat{\mathbf{x}}_{new} = \mathbf{QU}^T \mathbf{k}_{new}$ is the mode-change-related information, where \mathbf{U} is the score matrix of \mathbf{X} , $\mathbf{k}_{new} = \mathbf{K}(\mathbf{E}, \mathbf{e}_{new}^T)$ is the new kernel vector, and $\mathbf{t}_{new} = \mathbf{U}^T \mathbf{k}_{new}$ is the new score of \mathbf{x}_{new} .

2) The new score of $\tilde{\mathbf{x}}_{new}$ is computed as:

$$\mathbf{t}_{new,x} = \mathbf{U}_x^T \mathbf{k}_{new,x} \quad (8)$$

Here, \mathbf{U}_x is the score matrix of \mathbf{F}_x , and $\mathbf{k}_{new,x} = \mathbf{K}(\mathbf{F}_x, \tilde{\mathbf{x}}_{new}^T)$.

3) The corresponding detection statistics (T^2 and Q) of the principal component subspace (PCS) and residual subspace (RS) are computed [36].

III. IMPROVED NONLINEAR EXTERNAL ANALYSIS REGRESSION (INEAR) MODEL

In this section, two external models based on KOPLS is first established. To achieve fault detection, an IPLS-based internal regression model between the residual information in the main variables and that in the quality variables is established. Fig. 1 shows the principle of the established INEAR model.

A. EXTERNAL MODEL

We consider historical data $\mathbf{H} \in \mathbf{R}^{n \times c}$, where n and c represent the numbers of samples and process variables, respectively, and $n \gg c$. Based on an external analysis, \mathbf{H} can be divided into three parts: external variables $\mathbf{E} \in \mathbf{R}^{n \times c_e}$, main variables $\mathbf{X} \in \mathbf{R}^{n \times c_x}$, and quality variables $\mathbf{Y} \in \mathbf{R}^{n \times c_y}$, where $c_e + c_x + c_y = c$.

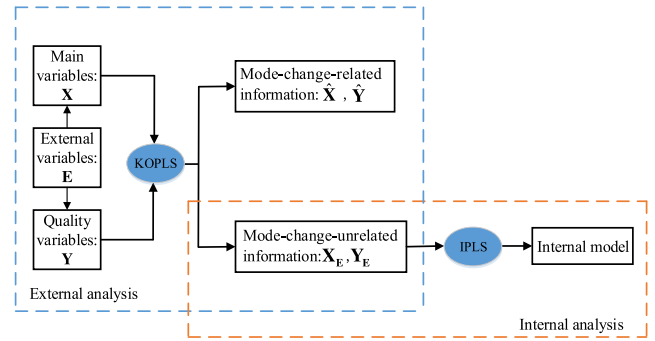


FIGURE 1. Overview of INEAR algorithm.

To separate input-related (i.e., mode-change-related) information in \mathbf{X} and \mathbf{Y} , a regression model between \mathbf{E} and \mathbf{X}/\mathbf{Y} is established. Although the existing nonlinear regression algorithms have similar steps in extracting input-related information, KOPLS is more advantageous. Compared with other algorithms, KOPLS requires a smaller number of loadings. The KOPLS model is easier to understand and interpret. In addition, in the external model, the mode-change-related information only needs to be removed, without being analyzed in detail. Therefore, KOPLS is utilized to develop the external regression model.

In this method, \mathbf{E} and \mathbf{X} are regarded as input and output, respectively, and the correlation between them is analyzed by KOPLS [37]. The same is true for \mathbf{E} and \mathbf{Y} . As a result, the KOPLS model between the external and main variables is given as:

$$\begin{cases} \Phi(\mathbf{E}) = \hat{\Phi}_x(\mathbf{E}) + \tilde{\Phi}_x(\mathbf{E}) \\ \mathbf{X} = \mathbf{T}_{x,p} \left(\mathbf{T}_{x,p}^T \mathbf{T}_{x,p} \right)^{-1} \mathbf{T}_{x,p}^T \mathbf{T}_x \mathbf{P}_x^T + \mathbf{X}_E \end{cases} \quad (9)$$

Here, $\hat{\Phi}_x(\mathbf{E})$ and $\tilde{\Phi}_x(\mathbf{E})$ are the principal and residual information of $\Phi(\mathbf{E})$, respectively, which are orthogonal to each other; $\hat{\mathbf{X}} = \mathbf{T}_{x,p} \left(\mathbf{T}_{x,p}^T \mathbf{T}_{x,p} \right)^{-1} \mathbf{T}_{x,p}^T \mathbf{T}_x \mathbf{P}_x^T$ is the full information influenced by \mathbf{E} , where \mathbf{P}_x is the predictive loading matrix of \mathbf{X} composed of eigenvectors corresponding to the first C highest eigenvalues of $\mathbf{X}^T \mathbf{KX}$, $\mathbf{T}_x = \mathbf{XP}_x$ is the predictive score matrix of \mathbf{X} , and $\mathbf{T}_{x,p}$ is the predictive score of \mathbf{E} , which is similar to the final matrix of step 8 when calculating the correlation between \mathbf{E} and \mathbf{X} in Table 1. \mathbf{X}_E is the information uninfluenced by \mathbf{E} , i.e., mode-change-unrelated information, which is further analyzed to establish the fault detection model, as it is unrelated to the mode change.

Similarly, another KOPLS model between the external and quality variables is given as:

$$\begin{cases} \Phi(\mathbf{E}) = \hat{\Phi}_y(\mathbf{E}) + \tilde{\Phi}_y(\mathbf{E}) \\ \mathbf{Y} = \mathbf{T}_{y,p} \left(\mathbf{T}_{y,p}^T \mathbf{T}_{y,p} \right)^{-1} \mathbf{T}_{y,p}^T \mathbf{T}_y \mathbf{P}_y^T + \mathbf{Y}_E \end{cases} \quad (10)$$

Here, $\hat{\Phi}_y(\mathbf{E})$ and $\tilde{\Phi}_y(\mathbf{E})$ are the principal and residual information of $\Phi(\mathbf{E})$, respectively, which are orthogonal to each other; $\hat{\mathbf{Y}} = \mathbf{T}_{y,p} \left(\mathbf{T}_{y,p}^T \mathbf{T}_{y,p} \right)^{-1} \mathbf{T}_{y,p}^T \mathbf{T}_y \mathbf{P}_y^T$ is the full

TABLE 1. KOPLS algorithm [37].

Step	Description	Computation	Dimension
1	Compute predictive components by eigenvalue decomposition, and extract A eigenvectors corresponding to the A largest eigenvalues	$(\mathbf{P}_y, \Lambda) \leftarrow \text{EVD}(\mathbf{Y}^T \mathbf{K} \mathbf{Y}, A)$	$[c_y \times A]$
2	Compute predictive score matrix of \mathbf{Y}	$\mathbf{T}_y = \mathbf{Y} \mathbf{P}_y$	$[n \times A]$
3	Compute predictive score matrix of \mathbf{E}	$\mathbf{T}_{E_y} = \mathbf{K} \mathbf{T}_y \Lambda^{-1/2}$	$[n \times A]$
4	Compute \mathbf{Y} -orthogonal loading of \mathbf{E} , $\mathbf{K}_{b,1}$ and \mathbf{T}_1 are originally defined as \mathbf{K} and \mathbf{T}_{E_y} , respectively	$(\mathbf{p}_{o,i}, \Lambda_{o,i}) \leftarrow \text{EVD}(\mathbf{T}_i^T (\mathbf{K}_{b,i} - \mathbf{T}_i \mathbf{T}_i^T) \mathbf{T}_i, 1), i \geq 1$	$[A \times 1]$
5	Compute \mathbf{Y} -orthogonal score vector of \mathbf{E}	$\mathbf{t}_{o,i} = (\mathbf{K}_{b,i} - \mathbf{T}_i \mathbf{T}_i^T) \mathbf{T}_i \mathbf{p}_{o,i} \Lambda_{o,i}^{-1/2}$	$[n \times 1]$
6	Deflate \mathbf{K} ,	$\mathbf{K}_{i+1} = \mathbf{K}_i (\mathbf{I} - \mathbf{t}_{o,i} \mathbf{t}_{o,i}^T)$	$[n \times n]$
7	Deflate $\mathbf{K}_{b,i}$	$\mathbf{K}_{b,i+1} = (\mathbf{I} - \mathbf{t}_{o,i} \mathbf{t}_{o,i}^T) \mathbf{K}_{b,i} (\mathbf{I} - \mathbf{t}_{o,i} \mathbf{t}_{o,i}^T)$	$[n \times n]$
8	Update predictive score of \mathbf{E}	$\mathbf{T}_{i+1} = \mathbf{K}_{i+1} \mathbf{T}_y \Lambda^{-1/2}$	$[n \times A]$
9	The step (4) to (8) is repeated to obtain all \mathbf{Y} -orthogonal information	The step (4) to (8) is repeated to obtain all \mathbf{Y} -orthogonal information	
10	Compute predictive score of \mathbf{E}_{new} , m is the number of online samples	$\mathbf{T}_{new,y} = \mathbf{K}_{new,y} \mathbf{T}_y \Lambda^{-1/2}$	$[m \times A]$
11	Compute predictable \mathbf{Y}_{new} and $\mathbf{T}_{y,p}$ is the final matrix of step (8)	$\hat{\mathbf{Y}}_{new} = \mathbf{T}_{new,y} (\mathbf{T}_{y,p}^T \mathbf{T}_{y,p})^{-1} \mathbf{T}_{y,p}^T \mathbf{T}_y \mathbf{P}_y^T$	$[m \times c_y]$

information influenced by \mathbf{E} , where \mathbf{P}_y , \mathbf{T}_y , and $\mathbf{T}_{y,p}$ are the predictive loading matrix of \mathbf{Y} , predictive score matrix of \mathbf{Y} , and predictive score matrix of \mathbf{E} , respectively, as shown in Table 1. \mathbf{Y}_E is the information uninfluenced by \mathbf{E} , i.e., mode-change-unrelated information, which is further analyzed to establish the fault detection model. It is worth noting that the specific information of \mathbf{X}_E and \mathbf{Y}_E may be different, as they are obtained based on different model structures.

So far, the mode-change-related information in \mathbf{X} and \mathbf{Y} is completely removed, and the remaining information (i.e. \mathbf{X}_E and \mathbf{Y}_E) has no relation with mode change. This means that the correlation analysis between \mathbf{X}_E and \mathbf{Y}_E is performed under a single mode, which can reduce the complexity of model, and improve the accuracy of model. Next, the regression model (that is, internal model) between \mathbf{X}_E and \mathbf{Y}_E needs to be accurately built to achieve process detection.

B. INTERNAL MODEL

Compared with OPLS, IPLS is more advantageous in separating output-related information and output-unrelated information, which is the main purpose of the internal model. Besides, IPLS can directly identify whether a fault is output-related based on the two detection statistics of the training model, whereas OPLS needs to further analyze the output-unrelated information.

\mathbf{X}_E and \mathbf{Y}_E are regarded as input and output, respectively. The internal model based on IPLS can be obtained as follows:

$$\begin{cases} \mathbf{X}_E = \mathbf{T}_{E1} \mathbf{P}_{E1}^T + \mathbf{T}_{E2} \mathbf{P}_{E2}^T \\ \mathbf{Y}_E = \mathbf{X}_E \mathbf{V}_E + \tilde{\mathbf{Y}}_E \end{cases} \quad (11)$$

Here, $\mathbf{V}_E \in \mathbf{R}^{c_x \times c_y}$ is the regression coefficient matrix between \mathbf{X}_E and \mathbf{Y}_E ; $\mathbf{P}_{E1} \in \mathbf{R}^{c_x \times q_x}$ and $\mathbf{P}_{E2} \in \mathbf{R}^{c_x \times (c_x - q_x)}$ are the loading matrices of PCS and RS of \mathbf{X}_E , respectively; $\mathbf{T}_{E1} \in \mathbf{R}^{n \times q_x}$ and $\mathbf{T}_{E2} \in \mathbf{R}^{n \times (c_x - q_x)}$ are the score matrices of PCS and RS of \mathbf{X}_E , respectively; $\tilde{\mathbf{Y}}_E$ is the residual of \mathbf{Y}_E ; and q_x is the number of loadings. Based on the above analysis, the faults occurring in a multimode process, can be detected based on the appropriate detection scheme, which is introduced in the next section.

IV. FAULT DETECTION BASED ON INNERAR

Online data $e_{new} \in \mathbf{R}^{c_e}$ and $\mathbf{x}_{new} \in \mathbf{R}^{c_x}$ are first preprocessed to remove the mode-change-related information in \mathbf{x}_{new} , and then, the operating status is detected based on the detection statistics computed from the mode-change-unrelated information in \mathbf{x}_{new} . Based on KOPLS (Eq. (9)), mode-change-related information in \mathbf{x}_{new} can be computed:

$$\hat{\mathbf{x}}_{new} = \left[(\mathbf{T}_{x,p}^T \mathbf{T}_{x,p})^{-1} \mathbf{T}_{x,p}^T \mathbf{T}_x \mathbf{P}_x^T \right]^T \mathbf{t}_{new,x} \quad (12)$$

Here, $\mathbf{t}_{new,x} = (\mathbf{T}_x \Lambda_x^{-1/2})^T k_{new,x} \in \mathbf{R}^{C \times 1}$ is the predictive score of e_{new} , and $k_{new,x} \in \mathbf{R}^n$ is the new kernel vector [37].

The mode-change-unrelated information in \mathbf{x}_{new} can be computed as:

$$\mathbf{x}_{E,new} = \mathbf{x}_{new} - \hat{\mathbf{x}}_{new} \quad (13)$$

Finally, the detection statistics can be computed as:

$$T_p^2 = \mathbf{t}_p^T \left(\frac{\mathbf{T}_{E_1}^T \mathbf{T}_{E_1}}{n-1} \right)^{-1} \mathbf{t}_p = \left(\mathbf{P}_{E_1}^T \mathbf{x}_{E,new} \right)^T \times \left(\frac{\mathbf{T}_{E_1}^T \mathbf{T}_{E_1}}{n-1} \right)^{-1} \mathbf{P}_{E_1}^T \mathbf{x}_{E,new} \quad (14)$$

$$T_r^2 = \mathbf{t}_r^T \left(\frac{\mathbf{T}_{E_2}^T \mathbf{T}_{E_2}}{n-1} \right)^{-1} \mathbf{t}_r = \left(\mathbf{P}_{E_2}^T \mathbf{x}_{E,new} \right)^T \times \left(\frac{\mathbf{T}_{E_2}^T \mathbf{T}_{E_2}}{n-1} \right)^{-1} \mathbf{P}_{E_2}^T \mathbf{x}_{E,new} \quad (15)$$

Here, $\mathbf{t}_p = \mathbf{P}_{E_1}^T \mathbf{x}_{E,new}$ and $\mathbf{t}_r = \mathbf{P}_{E_2}^T \mathbf{x}_{E,new}$ are the new score vectors of PCS and RS of $\mathbf{x}_{E,new}$, respectively.

Based on above computation, it can be known that mode-change-related information of online data must be removed first, which ensures that the establishment of detection statistics is similar to that under the single mode. Therefore, mode change can be distinguished from process faults, and the fault detection can be achieved whether the mode change by the proposed detection scheme. As worthy of mention, PCA [44] can be performed on $\hat{\mathbf{X}}/\hat{\mathbf{Y}}$ to establish the corresponding detection statistics (T^2 and Q) to detect the mode-change-related faults. If either T^2 or Q is greater than or equal to the control limit, a mode-change-related fault is said to have occurred. Otherwise, mode-change-related variables are normal, and the following detection scheme is given.

As \mathbf{t}_p and \mathbf{t}_r contain output-related information and output-unrelated information, respectively, if T_p^2 is greater than or equal to the corresponding control limit [45]–[47], an output-related fault is said to have occurred; if T_p^2 is lower than the corresponding control limit and T_r^2 is greater than or equal to the corresponding control limit, an output-unrelated fault is said to have occurred; if both the statistics are lower than the corresponding control limit, the operational process is normal. Fig. 2 shows the flowchart of the fault detection scheme.

V. SIMULATION: PENICILLIN FERMENTATION PROCESS

Penicillin ferments under different operating modes when the initial conditions, set points, and/or pH, among others, are set differently. Therefore, the PFP [48], shown in Fig. 3, is a good representative example of a multimode process. It contains 17 process variables (Table 2) [49]. The hot water flow rate in the entire process is not considered when it is 0; the other 16 process variables are selected for detection. According to the operating conditions of Pensim V2.0, CO₂, pH, and temperature are highly related to mode change, and temperature is affected by cold-water flow rate that is related to outside of process. Therefore, CO₂, pH, and cold-water flow rate are selected as the external variables. During the PFP, both biomass and penicillin ferment in the culture volume, and they are affected by process variables [50]. In addition, although temperature is related to biomass

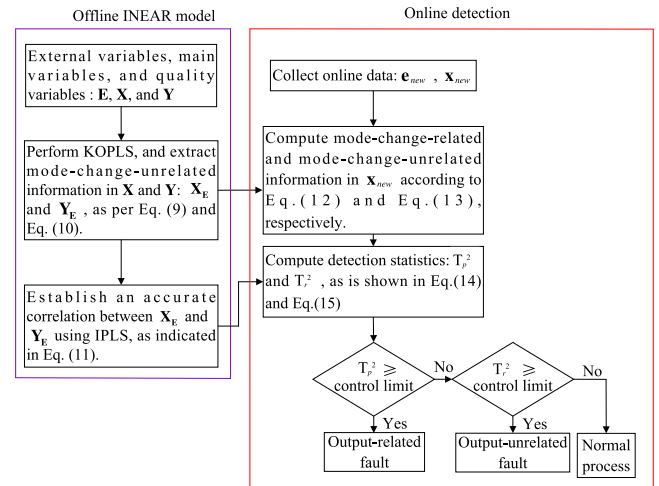


FIGURE 2. Flow chart of detection scheme based on INEAR.

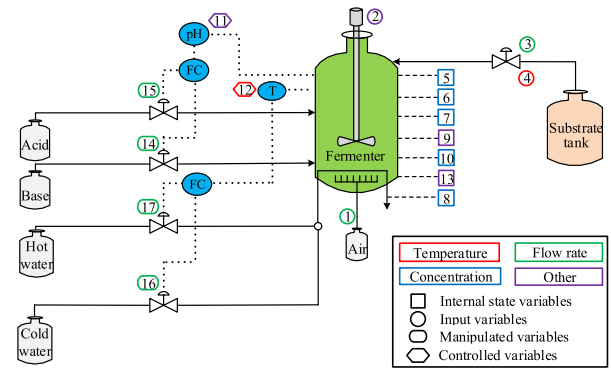


FIGURE 3. Penicillin fermentation process diagram.

TABLE 2. Description of variables [49].

No	Variable name	Unit
1	Aeration rate	L/h
2	Agitator power	W
3	Substrate feed rate	L/h
4	Substrate feed temperature	K
5	Substrate concentration	g/L
6	Dissolved oxygen	mmol/L
7	Biomass concentration	g/L
8	Penicillin concentration	g/L
9	Culture volume	L
10	CO ₂	mmol/L
11	pH	—
12	Temperature	K
13	Generated heat	kJ
14	Base water flow rate	mL/h
15	Acid water flow rate	mL/h
16	Cold water flow rate	L/h
17	Hot water flow rate	L/h

and penicillin, it is also directly affected by some process variables. As a result, the biomass concentration, culture volume, temperature, and penicillin concentration are selected as the quality variables. The rest are selected as the main variables.

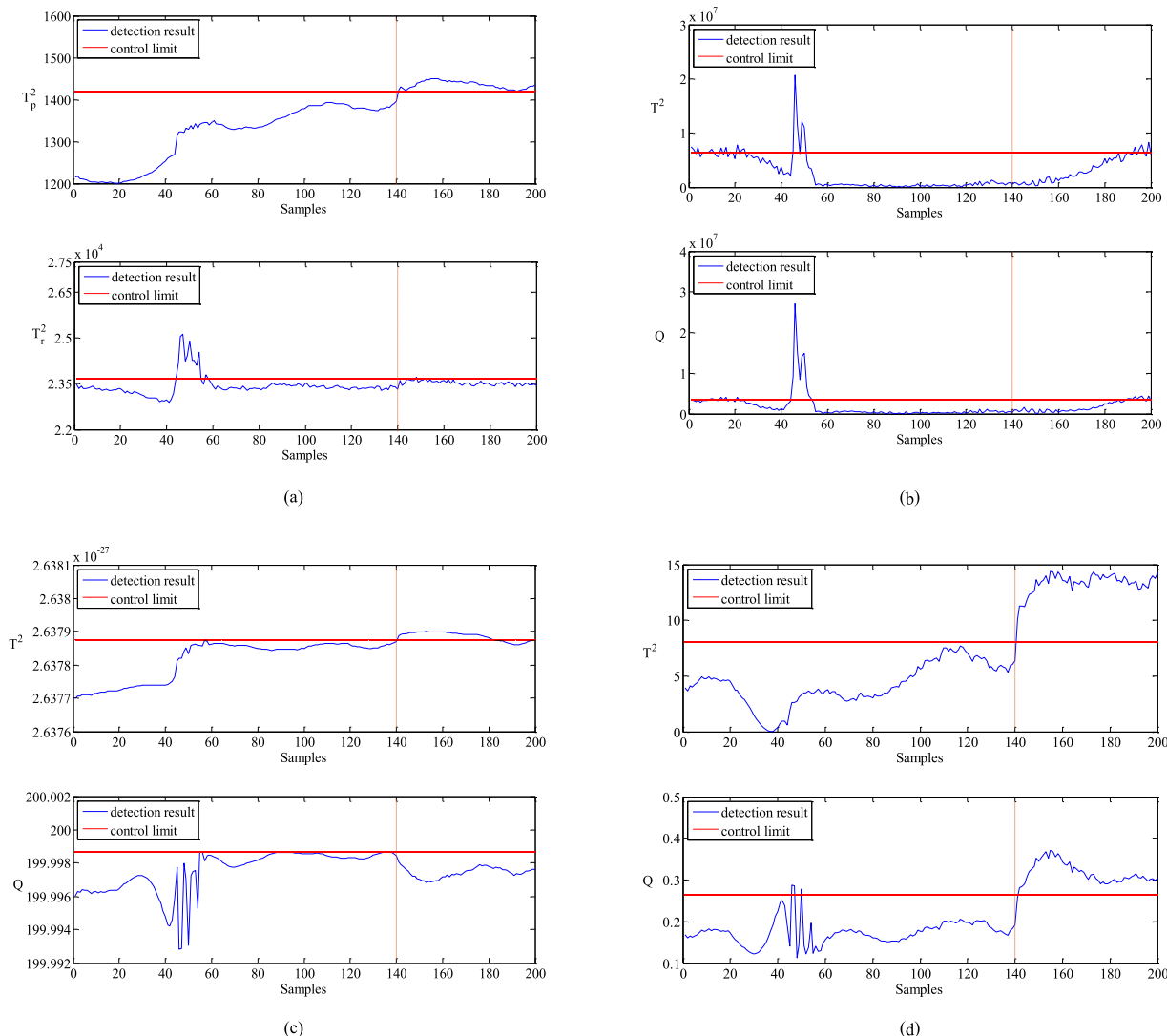


FIGURE 4. Detection results of fault 1: (a) INEAR, (b) PLS-EAR, (c) KPLS-EAR, (d) KOPLS-EAR.

In this simulation, the data generated using Pensim V2.0 [51] includes two modes, namely mode 1 and mode 2, each of which contains 200 sample points. Table 3 lists the specific settings of the two modes. In addition, based on the purpose and applicability of the experiment, three types of faults were introduced. Fault 1 is a step fault of the substrate feed rate under mode 1. Faults 2 and 3 are step and ramp faults of the substrate feed rate under mode 2, respectively. The three faults occur in the 141st hour and remain until the end. The magnitude or slope of the above three faults are 0.5, 0.7, and 0.9, respectively. The above data are used to demonstrate the validity and stability of the proposed method by comparing with the PLS-based EAR (PLS-EAR) [33], KPLS-EAR [33], [43], and KOPLS-based EAR (KOPLS-EAR) [33], [37].

Figs. 4, 5, and 6 show comparisons of the above four methods when the slope or magnitude of the above three faults is 0.7. Mode 1 is used as the training mode. Based on the cross-validation, both the loadings of the external

TABLE 3. Description of the two modes.

Mode	Initial conditions	Set points	Temperature	pH
1	Default	Default	Closed loop	PID (Closed loop)
2	Default	Default	Closed loop	On-off

model, as shown in (9) and (10), are set to 2, and the loading of the internal model is set to 5. As comparative experiments, the corresponding loadings of PLS-EAR and KPLS-EAR are set to 2, 3, and 5, respectively. All the loadings of KOPLS-EAR are set to 1. These results show that the loadings of KOPLS are lower than that in the others. As there are only three external variables, the loading advantage of KOPLS in this simulation is not clearly reflected. However, studies [37], [52]–[53] have shown that the number of KOPLS loadings is significantly lower than that in other methods.

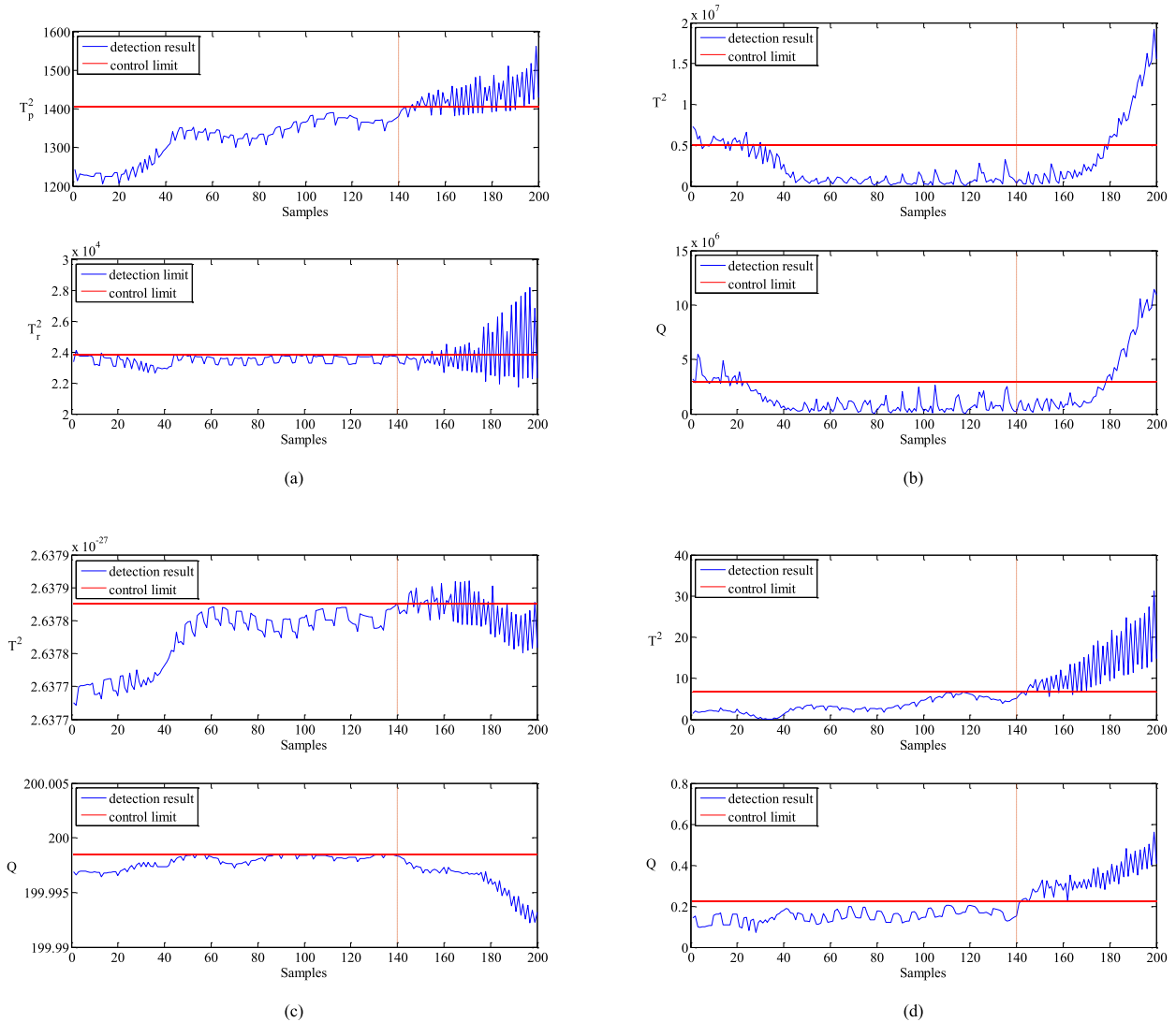


FIGURE 5. Detection results of fault 2: (a) INEAR, (b) PLS-EAR, (c) KPLS-EAR, (d) KOPLS-EAR.

Fig. 4(a) shows that although there are some false alarms between the 40th and 60th sample points, T_r^2 barely detects the fault 1. In addition, T_p^2 detects a step fault between the 141st and 200th sample points. This indicates that an output-related fault occurred under mode 1, which is also consistent with the fact. However, Fig. 4(b) shows that the fault is detected by T^2 and Q only between the last 10 sample points, and there is a certain false alarm. Therefore, the PLS-EAR cannot detect fault 1. Fig. 4(c) shows that only T^2 detects a step fault with some missing alarms, which demonstrates that INEAR performs more accurately although detection results of INEAR and KPLS-EAR are similar. Both detection statistics accurately detect a step fault using KOPS-EAR, as indicated in Fig. 4(d). Compared with INEAR, this illustrates that output-related and output-unrelated information had not been completely separated. The above results indicate that INEAR performs more accurately

and effectively for output-related faults under single mode process.

As shown in Fig. 5(a), a ramp fault is detected by T_p^2 from the 143th sample point until the end. Moreover, T_r^2 detects the fault with a large number of missing alarms, and it can even be considered that T_r^2 substantially fails to detect the fault. $\mathbf{P}_{E_1}^T \mathbf{P}_{E_2} \approx \mathbf{0}$ is taken in the actual simulation instead of the SVD-based theoretical result $\mathbf{P}_{E_1}^T \mathbf{P}_{E_2} = \mathbf{0}$. Therefore, there may be some output-related information in the output-unrelated subspace. As a result, T_r^2 has some alarms during the fault occurrence period. The above detection result also confirms the detection scheme given in Section IV: an output-related fault is determined only when T_p^2 is greater than the control limit. Fig. 5(b) shows the detection results of PLS-EAR. There are some missing and false alarms in T^2 and Q , and the detection results of the two statistics are similar, indicating that the mode-change-related information

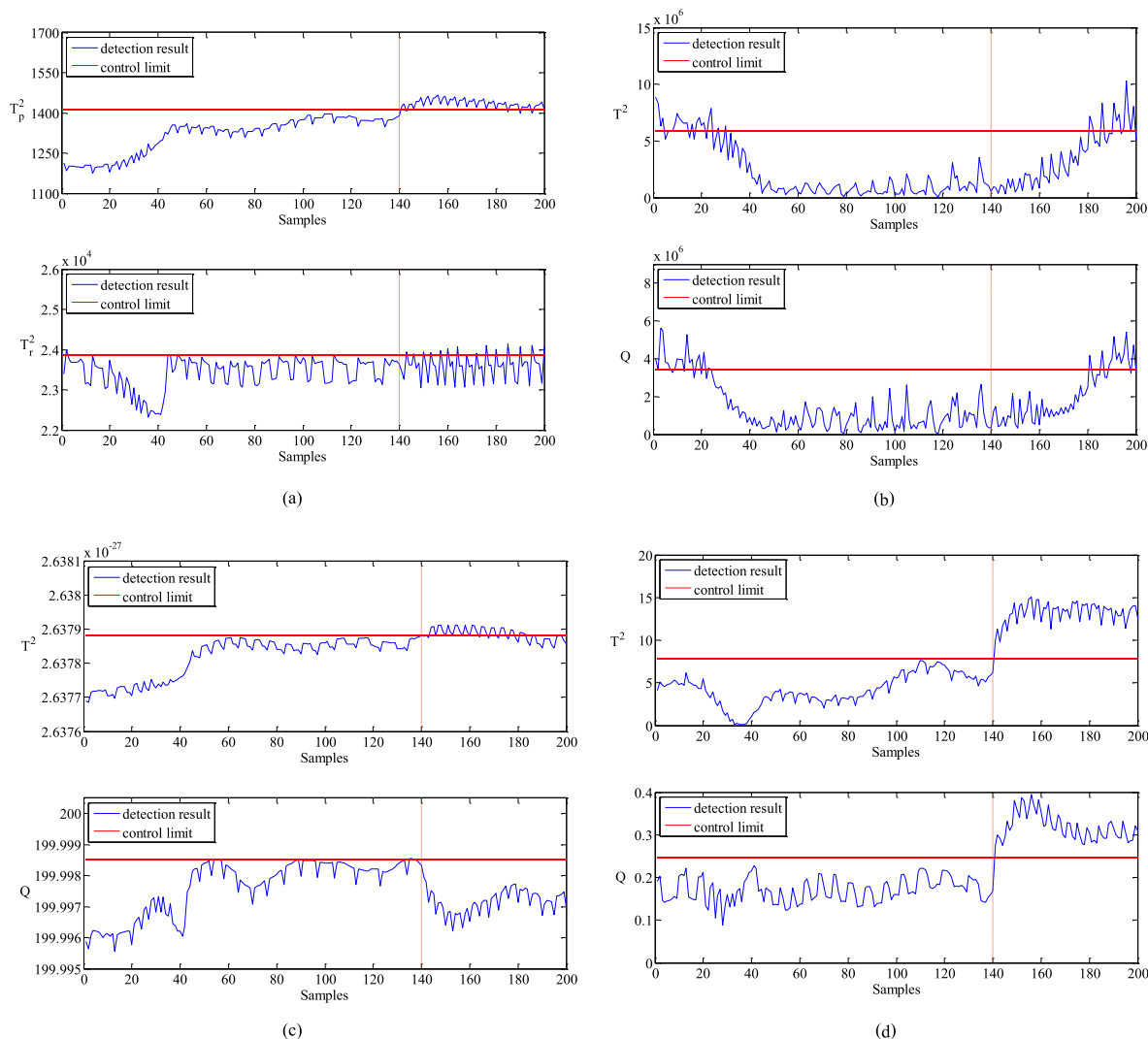


FIGURE 6. Detection results of fault 3: (a) INEAR, (b) PLS-EAR, (c) KPLS-EAR, (d) KOPLS-EAR.

had not been completely removed and that output-related and output-unrelated information had not been completely separated. Both detection statistics barely detect fault 2 using KPLS-EAR, as indicated in Fig. 5(c), which shows that this method loses the ability to detect fault 2. Fig. 5(d) shows fault 2 is effectively detected by T^2 and Q . The output-related and output-unrelated information had not been accurately separated although fault 2 is detected, which makes this method may not be able to effectively identify output-unrelated faults, as the output-unrelated fault will be mistaken for output-related fault once it is detected by T^2 . Therefore, we can conclude that INEAR outperforms the other three methods in detecting output-related faults in multimode processes.

As shown in Fig. 6(a), fault 3 is detected by T_p^2 , but is barely detected by T_r^2 , indicating that the step output-related fault of mode 2 is detected by the proposed method. For comparison, Fig. 6(b) shows that the fault is barely detected by T^2 and Q , and there are some false alarms at the beginning.

For KPLS-EAR and KOPLS-EAR, the detection results are similar to fault 1. Thereby, the above results prove that the proposed method can more accurately detect faults in multimode processes. Combined with the detection results of fault 1 and fault 2, the proposed method can not only accurately detect faults but can also effectively identify the different types of faults under different modes.

To demonstrate the multimode detection results of the four methods more accurately, the fault detection rates (FDRs) and false alarm rates (FARs) of the above three faults are given, as listed in Table 4 and Table 5, where INEAR keeps relatively high FDRs in output-related indicator T_p^2 for all consider faults, and simultaneously keeps very low FARs in both detection statistics. These results indicate that INEAR performs quite stable and accurate for output-related faults in multimode processes. Remarkably, the FDRs of fault 2 of T_p^2 are lower than those of the other two faults; this is due to the characteristics of fault 2. As we can

TABLE 4. FDRs of INEAR, PLS-EAR, KPLS-EAR, and KOPLS-EAR.

Fault number	Fault slope/magnitude	FDR (%)							
		INEAR		PLS-EAR		KPLS-EAR		KOPLS-EAR	
		T_p^2	T_r^2	T^2	Q	T^2	Q	T^2	Q
1	0.5	68.33	0	3.33	3.33	66.67	0	100	96.67
	0.7	98.33	3.33	11.67	13.33	71.67	0	100	98.33
	0.9	100	21.67	26.67	21.67	80	0	100	100
2	0.5	70	38.33	30	33.33	36.67	0	88.33	90
	0.7	66.67	35	36.67	36.67	41.67	0	88.33	93.33
	0.9	75	40	38.33	43.33	45	0	90	90
3	0.5	76.67	18.33	6.67	11.67	43.33	0	100	100
	0.7	90	25	16.67	20	56.67	0	100	100
	0.9	95	28.33	31.67	31.67	66.67	0	100	100

TABLE 5. FARs of INEAR, PLS-EAR, KPLS-EAR, and KOPLS-EAR.

Fault number	Fault slope/magnitude	FAR (%)							
		INEAR		PLS-EAR		KPLS-EAR		KOPLS-EAR	
		T_p^2	T_r^2	T^2	Q	T^2	Q	T^2	Q
1	0.5	0	7.86	18.57	12.14	0	3.33	0	5
	0.7	0	8.57	18.57	12.86	0	5	0	5
	0.9	0	8.57	18.57	12.14	0	5	0	5
2	0.5	0	2.86	13.57	12.86	0	3.33	0	0
	0.7	0	2.86	13.57	11.43	0	5	0	0
	0.9	0	2.86	13.57	11.43	0	5	0	0
3	0.5	0	2.86	14.29	13.57	0	3.33	0	0
	0.7	0	3.57	13.57	13.57	0	3.33	0	0
	0.9	0	2.86	13.57	12.86	0	3.33	0	0

know from PFP, fault 2 increases in a serrated shape, and some fault values are even lower than normal. In contrast, PLS-EAR has rather low (high) FDRs (FARs) in both detection statistics for all consider faults, and simultaneously the FDRs/FARs of both statistic are similar, which indicates that the faults are basically not detected. For KPLS-EAR, although FDRs of Q for all consider faults are 0, FDRs of T^2 are obviously lower than those of T_p^2 . In addition, except for fault 1, the FARs of Q are slightly more than T_r^2 . It can be concluded from these results that the detection ability of KPLS-EAR is weaker than INEAR. For KOPLS-EAR, FDRs (FARs) of both detection statistics are slightly greater than (lower than) those of T_p^2 and T_r^2 . However, the high FDRs of Q reveal the output-related and output-unrelated information had not been completely separated. The above comparisons demonstrate that INEAR outperforms PLS-EAR, KPLS-EAR, and KOPLS-EAR in stably and accurately determining the output-related faults occurring in multimode processes.

VI. CONCLUSION

In this paper, a new external model–internal model–detection structure is proposed, with INEAR as a new fault detection method for multimode processes. During the external modeling phase, KOPLS is applied to establish a regression model between the external and main/quality variables to accurately remove mode-change-related information. During the internal modeling phase, IPLS utilizes the full correlation between X_E and Y_E to establish the regression model, thus completely separating the output-related and output-unrelated information. Lastly, during the detection phase, faults can be accurately detected. PFP was considered as an application example, with its variables divided into external, main, and quality variables to detect different faults under two modes. The detection results show that the proposed method performs quite stably and accurately in detecting output-related faults in multimode processes.

This study only addresses the fault detection in multimode processes containing nonlinear external variables and linear

main and quality variables. The fault detection in multimode processes with all variables nonlinear and fault diagnosis using the INEAR deserve future work. Besides, in this simulation, mode-change-related information is defaulted to normal, as the faults of CO₂, pH, and cold-water flow rate cannot be given by Pensim V2.0. However, it is often abnormal in some industry processes, which will bring some bad consequences. Thus, in the future work, the mode-change-related faults should be specifically analyzed and researched.

REFERENCES

- [1] S. Gajjar, M. Kulahci, and A. Palazoglu, "Real-time fault detection and diagnosis using sparse principal component analysis," *J. Process Control*, vol. 67, pp. 112–128, Jul. 2018, doi: [10.1016/j.jprocont.2017.03.005](https://doi.org/10.1016/j.jprocont.2017.03.005).
- [2] H. Zhao, J. Zheng, J. Xu, and W. Deng, "Fault diagnosis method based on principal component analysis and broad learning system," *IEEE Access*, vol. 7, pp. 99263–99272, 2019, doi: [10.1109/access.2019.2929094](https://doi.org/10.1109/access.2019.2929094).
- [3] V. S. Yellapu, V. Vajpayee, and A. P. Tiwari, "Online fault detection and isolation in advanced heavy water reactor using multiscale principal component analysis," *IEEE Trans. Nucl. Sci.*, vol. 66, no. 7, pp. 1790–1803, Jul. 2019, doi: [10.1109/tns.2019.2919414](https://doi.org/10.1109/tns.2019.2919414).
- [4] J. Camacho, R. Theron, J. M. Garcia-Gimenez, G. Macia-Fernandez, and P. Garcia-Teodoro, "Group-wise principal component analysis for exploratory intrusion detection," *IEEE Access*, vol. 7, pp. 113081–113093, 2019, doi: [10.1109/access.2019.2935154](https://doi.org/10.1109/access.2019.2935154).
- [5] D. H. Zhou, G. Li, and S. J. Qin, "Total projection to latent structures for process monitoring," *AICHE J.*, vol. 56, no. 1, pp. 168–178, Jan. 2010, doi: [10.1002/aic.11977](https://doi.org/10.1002/aic.11977).
- [6] S. J. Qin and Y. Zheng, "Quality-relevant and process-relevant fault monitoring with concurrent projection to latent structures," *AICHE J.*, vol. 59, no. 2, pp. 496–504, Feb. 2013, doi: [10.1002/aic.13959](https://doi.org/10.1002/aic.13959).
- [7] Z. Dong and N. Ma, "A novel nonlinear partial least square integrated with error-based extreme learning machine," *IEEE Access*, vol. 7, pp. 59903–59912, 2019, doi: [10.1109/access.2019.2911741](https://doi.org/10.1109/access.2019.2911741).
- [8] T. Lan, C. Tong, X. Chen, X. Shi, and Y. Chen, "KPI relevant and irrelevant fault monitoring with neighborhood component analysis and two-level PLS," *J. Franklin Inst.*, vol. 355, no. 16, pp. 8049–8064, Nov. 2018, doi: [10.1016/j.jfranklin.2018.07.016](https://doi.org/10.1016/j.jfranklin.2018.07.016).
- [9] X. Peng, Y. Tang, W. Du, and F. Qian, "Multimode process monitoring and fault detection: A sparse modeling and dictionary learning method," *IEEE Trans. Ind. Electron.*, vol. 64, no. 6, pp. 4866–4875, Jun. 2017, doi: [10.1109/tie.2017.2668987](https://doi.org/10.1109/tie.2017.2668987).
- [10] B. Song, S. Tan, and H. Shi, "Key principal components with recursive local outlier factor for multimode chemical process monitoring," *J. Process Control*, vol. 47, pp. 136–149, Nov. 2016, doi: [10.1016/j.jprocont.2016.09.006](https://doi.org/10.1016/j.jprocont.2016.09.006).
- [11] X. Deng, N. Zhong, and L. Wang, "Nonlinear multimode industrial process fault detection using modified kernel principal component analysis," *IEEE Access*, vol. 5, pp. 23121–23132, 2017, doi: [10.1109/access.2017.2764518](https://doi.org/10.1109/access.2017.2764518).
- [12] S. Li, X. Zhou, H. Shi, Z. Qiao, and Z. Zheng, "Monitoring of multimode processes based on subspace decomposition," *Ind. Eng. Chem. Res.*, vol. 54, no. 15, pp. 3855–3864, Apr. 2015, doi: [10.1021/ie504730x](https://doi.org/10.1021/ie504730x).
- [13] B. K. Flury, "Two generalizations of the common principal component model," *Biometrika*, vol. 74, no. 1, pp. 59–69, 1987, doi: [10.1093/biomet/74.1.59](https://doi.org/10.1093/biomet/74.1.59).
- [14] S. Lane, E. Martin, R. Kooijmans, and A. Morris, "Performance monitoring of a multi-product semi-batch process," *J. Process Control*, vol. 11, no. 1, pp. 1–11, Feb. 2001, doi: [10.1016/s0959-1524\(99\)00063-3](https://doi.org/10.1016/s0959-1524(99)00063-3).
- [15] D.-H. Hwang and C. Han, "Real-time monitoring for a process with multiple operating modes," *Control Eng. Pract.*, vol. 7, no. 7, pp. 891–902, Jul. 1999, doi: [10.1016/s0967-0661\(99\)00038-6](https://doi.org/10.1016/s0967-0661(99)00038-6).
- [16] T. Chen and J. Zhang, "On-line multivariate statistical monitoring of batch processes using Gaussian mixture model," *Comput. Chem. Eng.*, vol. 34, no. 4, pp. 500–507, Apr. 2010, doi: [10.1016/j.compchemeng.2009.08.007](https://doi.org/10.1016/j.compchemeng.2009.08.007).
- [17] Z. Ge and Z. Song, "Mixture Bayesian regularization method of PPCA for multimode process monitoring," *AICHE J.*, vol. 56, no. 11, pp. 2838–2849, Nov. 2010, doi: [10.1002/aic.12200](https://doi.org/10.1002/aic.12200).
- [18] X. Xie and H. Shi, "Dynamic multimode process modeling and monitoring using adaptive Gaussian mixture models," *Ind. Eng. Chem. Res.*, vol. 51, no. 15, pp. 5497–5505, Apr. 2012, doi: [10.1021/ie202720y](https://doi.org/10.1021/ie202720y).
- [19] S. Zhang, F. Wang, S. Tan, S. Wang, and Y. Chang, "Novel monitoring strategy combining the advantages of the multiple modeling strategy and Gaussian mixture model for multimode processes," *Ind. Eng. Chem. Res.*, vol. 54, no. 47, pp. 11866–11880, Dec. 2015, doi: [10.1021/acs.iecr.5b00373](https://doi.org/10.1021/acs.iecr.5b00373).
- [20] S. W. Choi, E. B. Martin, A. J. Morris, and I.-B. Lee, "Adaptive multivariate statistical process control for monitoring time-varying processes," *Ind. Eng. Chem. Res.*, vol. 45, no. 9, pp. 3108–3118, Apr. 2006, doi: [10.1021/ie050391w](https://doi.org/10.1021/ie050391w).
- [21] Y.-H. Lee, H. D. Jin, and C. Han, "On-line process state classification for adaptive monitoring," *Ind. Eng. Chem. Res.*, vol. 45, no. 9, pp. 3095–3107, Apr. 2006, doi: [10.1021/ie048969+](https://doi.org/10.1021/ie048969+).
- [22] S. J. Zhao, J. Zhang, and Y. M. Xu, "Monitoring of processes with multiple operating modes through multiple principle component analysis models," *Ind. Eng. Chem. Res.*, vol. 43, no. 22, pp. 7025–7035, Oct. 2004, doi: [10.1021/ie0497893](https://doi.org/10.1021/ie0497893).
- [23] S. J. Zhao, J. Zhang, and Y. M. Xu, "Performance monitoring of processes with multiple operating modes through multiple PLS models," *J. Process Control*, vol. 16, no. 7, pp. 763–772, Aug. 2006, doi: [10.1016/j.jprocont.2005.12.002](https://doi.org/10.1016/j.jprocont.2005.12.002).
- [24] C. Zhao, W. Wang, Y. Qin, and F. Gao, "Comprehensive subspace decomposition with analysis of between-mode relative changes for multimode process monitoring," *Ind. Eng. Chem. Res.*, vol. 54, no. 12, pp. 3154–3166, Apr. 2015, doi: [10.1021/ie504380c](https://doi.org/10.1021/ie504380c).
- [25] J. Yu and S. J. Qin, "Multimode process monitoring with Bayesian inference-based finite Gaussian mixture models," *AICHE J.*, vol. 54, no. 7, pp. 1811–1829, Jul. 2008, doi: [10.1002/aic.11515](https://doi.org/10.1002/aic.11515).
- [26] C. Tong, A. Palazoglu, and X. Yan, "An adaptive multimode process monitoring strategy based on mode clustering and mode unfolding," *J. Process Control*, vol. 23, no. 10, pp. 1497–1507, Nov. 2013, doi: [10.1016/j.jprocont.2013.09.017](https://doi.org/10.1016/j.jprocont.2013.09.017).
- [27] A. Haghani, T. Jeansch, and S. X. Ding, "Quality-related fault detection in industrial multimode dynamic processes," *IEEE Trans. Ind. Electron.*, vol. 61, no. 11, pp. 6446–6453, Nov. 2014, doi: [10.1109/tie.2014.2311409](https://doi.org/10.1109/tie.2014.2311409).
- [28] Y. Ma and H. Shi, "Multimode process monitoring based on aligned mixture factor analysis," *Ind. Eng. Chem. Res.*, vol. 53, no. 2, pp. 786–799, Jan. 2014, doi: [10.1021/ie4040797](https://doi.org/10.1021/ie4040797).
- [29] J. Yu, "Hidden Markov models combining local and global information for nonlinear and multimodal process monitoring," *J. Process Control*, vol. 20, no. 3, pp. 344–359, Mar. 2010, doi: [10.1016/j.jprocont.2009.12.002](https://doi.org/10.1016/j.jprocont.2009.12.002).
- [30] M. M. Rashid and J. Yu, "Hidden Markov model based adaptive independent component analysis approach for complex chemical process monitoring and fault detection," *Ind. Eng. Chem. Res.*, vol. 51, no. 15, pp. 5506–5514, Apr. 2012, doi: [10.1021/ie300203u](https://doi.org/10.1021/ie300203u).
- [31] M. Kano, S. Hasebe, I. Hashimoto, and H. Ohno, "Evolution of multivariate statistical process control: Application of independent component analysis and external analysis," *Comput. Chem. Eng.*, vol. 28, nos. 6–7, pp. 1157–1166, Jun. 2004, doi: [10.1016/j.compchemeng.2003.09.011](https://doi.org/10.1016/j.compchemeng.2003.09.011).
- [32] Z. Ge, C. Yang, Z. Song, and H. Wang, "Robust online monitoring for multimode processes based on nonlinear external analysis," *Ind. Eng. Chem. Res.*, vol. 47, no. 14, pp. 4775–4783, Jul. 2008, doi: [10.1021/ie071304y](https://doi.org/10.1021/ie071304y).
- [33] Z. Ge, Z. Song, and M. Kano, "External analysis-based regression model for robust soft sensing of multimode chemical processes," *AICHE J.*, vol. 60, no. 1, pp. 136–147, Jan. 2014, doi: [10.1002/aic.14253](https://doi.org/10.1002/aic.14253).
- [34] Z. Ge, F. Gao, and Z. Song, "Mixture probabilistic PCR model for soft sensing of multimode processes," *Chemometrics Intell. Lab. Syst.*, vol. 105, no. 1, pp. 91–105, Jan. 2011, doi: [10.1016/j.chemolab.2010.11.004](https://doi.org/10.1016/j.chemolab.2010.11.004).
- [35] D. T. A. Nguyen, S. M. Rissanen, P. Julkunen, E. Kallioniemi, and P. A. Karjalainen, "Principal component regression on motor evoked potential in single-pulse transcranial magnetic stimulation," *IEEE Trans. Neural Syst. Rehabil. Eng.*, vol. 27, no. 8, pp. 1521–1528, Aug. 2019, doi: [10.1109/tnsre.2019.2923724](https://doi.org/10.1109/tnsre.2019.2923724).
- [36] K. Peng, K. Zhang, and G. Li, "Quality-related process monitoring based on total kernel PLS model and its industrial application," *Math. Problems Eng.*, vol. 2013, pp. 1–14, Oct. 2013, doi: [10.1155/2013/707953](https://doi.org/10.1155/2013/707953).
- [37] M. Rantalainen, M. Bylesjö, O. Cloarec, J. K. Nicholson, E. Holmes, and J. Trygg, "Kernel-based orthogonal projections to latent structures (K-OPLS)," *J. Chemometrics*, vol. 21, nos. 7–9, pp. 376–385, Jul. 2007, doi: [10.1002/cem.1071](https://doi.org/10.1002/cem.1071).

- [38] X. F. Yuan, B. Huang, Y. L. Wang, C. H. Yang, and W. H. Gui, "Deep learning based feature representation and its application for soft sensor modeling with variable-wise weighted SAE," *IEEE Trans. Ind. Informat.*, vol. 14, no. 7, pp. 3235–3243, Jul. 2018, doi: [10.1109/tii.2018.2809730](https://doi.org/10.1109/tii.2018.2809730).
- [39] X. Yuan, J. Zhou, B. Huang, Y. Wang, C. Yang, and W. Gui, "Hierarchical quality-relevant feature representation for soft sensor modeling: A novel deep learning strategy," *IEEE Trans. Ind. Informat.*, to be published, doi: [10.1109/tii.2019.2938890](https://doi.org/10.1109/tii.2019.2938890).
- [40] X. Yuan, L. Li, and Y. Wang, "Nonlinear dynamic soft sensor modeling with supervised long short-term memory network," *IEEE Trans. Ind. Informat.*, to be published, doi: [10.1109/tii.2019.2902129](https://doi.org/10.1109/tii.2019.2902129).
- [41] Y. L. Wang, Z. F. Pan, X. F. Yuan, C. H. Yang, and W. H. Gui, "A novel deep learning based fault diagnosis approach for chemical process with extended deep belief network," *ISA Trans.*, to be published, doi: [10.1016/j.isatra.2019.07.001](https://doi.org/10.1016/j.isatra.2019.07.001).
- [42] S. Yin, X. Zhu, and O. Kaynak, "Improved PLS focused on key-performance-indicator-related fault diagnosis," *IEEE Trans. Ind. Electron.*, vol. 62, no. 3, pp. 1651–1658, Mar. 2015, doi: [10.1109/tie.2014.2345331](https://doi.org/10.1109/tie.2014.2345331).
- [43] F. Lindgren, P. Geladi, and S. Wold, "The kernel algorithm for PLS," *J. Chemometrics*, vol. 7, no. 1, pp. 45–59, Jan. 1993, doi: [10.1002/cem.1180070104](https://doi.org/10.1002/cem.1180070104).
- [44] Y. W. Zhang, *Jiyu Shuju de Fuza Gongye Guocheng Jiance*. Shenyang, China: Northeastern Univ. Press (in Chinese), 2011, pp. 36–40.
- [45] J.-M. Lee, C. Yoo, and I.-B. Lee, "Statistical process monitoring with independent component analysis," *J. Process Control*, vol. 14, no. 5, pp. 467–485, Aug. 2004, doi: [10.1016/j.jprocont.2003.09.004](https://doi.org/10.1016/j.jprocont.2003.09.004).
- [46] X. Hong, J. Gao, S. Chen, and T. Zia, "Sparse density estimation on the multinomial manifold," *IEEE Trans. Neural Netw. Learn. Syst.*, vol. 26, no. 11, pp. 2972–2977, Nov. 2015, doi: [10.1109/tnnls.2015.2389273](https://doi.org/10.1109/tnnls.2015.2389273).
- [47] X. Deng, X. Tian, and S. Chen, "Modified kernel principal component analysis based on local structure analysis and its application to nonlinear process fault diagnosis," *Chemometrics Intell. Lab. Syst.*, vol. 127, pp. 195–209, Aug. 2013, doi: [10.1016/j.chemolab.2013.07.001](https://doi.org/10.1016/j.chemolab.2013.07.001).
- [48] Y. Shu and J. Zhao, "Fault diagnosis of chemical processes using artificial immune system with vaccine transplant," *Ind. Eng. Chem. Res.*, vol. 55, no. 12, pp. 3360–3371, Mar. 2016, doi: [10.1021/acs.iecr.5b02646](https://doi.org/10.1021/acs.iecr.5b02646).
- [49] J.-M. Lee, C. Yoo, and I.-B. Lee, "On-line batch process monitoring using a consecutively updated multiway principal component analysis model," *Comput. Chem. Eng.*, vol. 27, no. 12, pp. 1903–1912, Dec. 2003, doi: [10.1016/s0098-1354\(03\)00151-0](https://doi.org/10.1016/s0098-1354(03)00151-0).
- [50] Y. Liu and H. Q. Wang, "Pensim simulator and its application in penicillin fermentation process," *J. Syst. Simul.*, vol. 18, no. 12, pp. 3524–3527, Dec. 2006, doi: [10.16182/j.cnki.joss.2006.12.049](https://doi.org/10.16182/j.cnki.joss.2006.12.049).
- [51] G. Birol, C. Ündey, and A. Çınar, "A modular simulation package for fed-batch fermentation: Penicillin production," *Comput. Chem. Eng.*, vol. 26, no. 11, pp. 1553–1565, Nov. 2002, doi: [10.1016/s0098-1354\(02\)00127-8](https://doi.org/10.1016/s0098-1354(02)00127-8).
- [52] M. Jalali-Heravi, H. Ebrahimi-Najafabadi, and A. Khodabandehloo, "Use of kernel orthogonal projection to latent structure in modeling of retention indices of pesticides," *QSAR Comb. Sci.*, vol. 28, nos. 11–12, pp. 1432–1441, Dec. 2009, doi: [10.1002/qsar.200910072](https://doi.org/10.1002/qsar.200910072).
- [53] E. L. Russell, L. H. Chiang, and R. D. Braatz, "Fault detection in industrial processes using canonical variate analysis and dynamic principal component analysis," *Chemometrics Intell. Lab. Syst.*, vol. 51, no. 1, pp. 81–93, May 2000, doi: [10.1016/s0169-7439\(00\)00058-7](https://doi.org/10.1016/s0169-7439(00)00058-7).



RONGRONG SUN received the M.S. degree from the College of Information Science and Engineering, Northeastern University, Shenyang, China, in 2015, where she is currently pursuing the Ph.D. degree. Her current research interests include data analysis, fault detection and diagnosis, and process control.

• • •